

AperTO - Archivio Istituzionale Open Access dell'Università di Torino

THORONDOR: a software for fast treatment and analysis of low-energy XAS data

This is the author's manuscript

Original Citation:

Availability:

This version is available <http://hdl.handle.net/2318/1761237> since 2020-11-04T16:06:40Z

Published version:

DOI:10.1107/S1600577520011388

Terms of use:

Open Access

Anyone can freely access the full text of works made available as "Open Access". Works made available under a Creative Commons license can be used according to the terms and conditions of said license. Use of all other works requires consent of the right holder (author or publisher) if not exempted from copyright protection by the applicable law.

(Article begins on next page)

THORONDOR: a software for quick treatment and analysis for low energy XAS data

David Horst Simonne^{a*}, Andrea Martini^{ab*}, Matteo Signorile^a, Alessandro Piovano^a, Luca Braglia^c, Piero Torelli^c, Elisa Borfecchia^a and Gabriele Ricchiardi^a

^aDepartment of Chemistry, INSTM Reference Center and NIS and CrisDi Interdepartmental Centers, University of Torino, Via P. Giuria 7, Torino, 10125, Italy

^bThe Smart Materials Research Center, Southern Federal University, Sladkova 178/24, Rostov-on-Don, 344090, Russian Federation

^cCNR-IOM, TASC Laboratory, S.S. 14 km 163.5, Trieste, Italy, 34149

Correspondence email: david.simonne@unito.it; andrea.martini@unito.it

THORONDOR is a Python software realized for the analysis of multiple NEXAFS spectra collected under *in situ* conditions. It allows the correction and normalization of the acquired spectra through a quick and intuitive interface. Moreover, it offers a sophisticated toolbox for the fitting of the NEXAFS rising edge peaks.

Abstract

THORONDOR is a data treatment software with graphic user interface (GUI) accessible via the browser-based Jupyter notebook framework (Kluyver, 2016). It aims to provide an interactive and user-friendly tool for the analysis of NEXAFS spectra collected during *in situ* experiments. The program allows on the fly representation and quick correction of large set of data coming from single or multiple experiments. In particular, it provides the possibility to align in energy several spectral profiles on the basis of user-defined references. Various techniques to realize background subtraction and signal normalization are made available. In this context, an innovation of this GUI consists in the usage of a slider-based approach that gives to the user the possibility to instantly manipulate and visualize the processed data. Finally, the program is characterized by an advanced fitting toolbox based on the *lmfit* package (Newville, 2014). It offers a large selection of fitting routines as well as different peak distributions and empirical ionization potential step edges, which can be used for the fit of the NEXAFS rising edge peaks. Statistical parameters describing the goodness of a fit, such as the chi-square or the R-factor together with the parameter uncertainties distributions and the related correlations can be extracted for each chosen model.

Keywords: NEXAFS; *in situ* measurements; data treatment; peak fitting; Graphical User Interface; Python.

1. Introduction

X-ray Absorption Spectroscopy (XAS) is a powerful tool for the characterization of a large variety of materials thanks to its chemical selectivity and high sensitivity in determining interatomic distance. Moreover, this technique can simultaneously provide information on the electronic and local structural properties of the systems under study, clarifying the relation between their atomic/electronic structure and their physicochemical properties (Mino *et al.*, 2013). These facts render this technique powerful to study surface/interface phenomena such as those found in heterogeneous catalysis, fuel cells or batteries (Guda *et al.*, 2019; Lassalle-Kaiser *et al.*, 2017). In these contexts, the usage of soft X-rays below 2.0 keV is extremely useful to study the oxidation state and the coordination geometry of both light element (at K-edges) and transition metals (at e.g. L-edges), which play a fundamental role in these fields (Tamenori, 2013).

In the soft X-ray energy regime, the high X-ray absorption coefficients make it often necessary to work under low-pressure environments (Stöhr, 1992). Although the high-vacuum condition produces an ideally clean environment for the sample under study, a multitude of chemically relevant phenomena take place only under ambient pressure (Castan-Guerrero *et al.*, 2018; Escudero *et al.*, 2013). In an effort to bridge the pressure gap in this context, different gas and liquid cells were designed in recent years, enabling to carry out soft X-ray studies of different reactions under *in situ* conditions (Blum *et al.*, 2009; Castan-Guerrero *et al.*, 2018; Escudero *et al.*, 2013; Forsberg *et al.*, 2007; Fuchs *et al.*, 2008; Guo & Luo, 2010; Havecker *et al.*, 1999; Knop-Gericke *et al.*, 1998; Tamenori, 2013; Tokushima *et al.*, 2009; Zheng *et al.*, 2011; Beaumont, 2020). In general, their design implies that the X-ray beam penetrates inside the reaction volume through a Si₃N₄ membrane of few tens of nanometres of thickness (Castan-Guerrero *et al.*, 2018). These membranes have sufficient mechanical resistance to resist the difference of pressure between the vacuum of the chamber, where the cell is situated, and the gas environment inside it, at atmospheric pressure (Escudero *et al.*, 2013). Because of the high yield of the photoelectric effect in the soft X-ray range and pushed by the experimental simplicity, the so called Total Electron Yield measured by the replacement current (or drain current) has emerged as the most popular way to perform XAS in the soft X-ray range (below 2 keV). This technique combines surface sensitivity, resulting from the short escape depth of photoelectrons in this energy range, and the practical advantage of minimizing the alignment problems with the detector (Escudero *et al.*, 2013). The standard way to acquire the absorption spectrum is realised by moving the monochromator with a discrete step, recording the TEY intensity at the selected energy, and repeating this operation for the entire energy range of interest. Recently, the experimental practice has been improved by continuously scanning the grating monochromator through the desired energy range (and sometimes also the undulator gap) while collecting the signal in a streaming mode. This last methodology, sometimes known as “fast-scan” or “on the fly scan”, significantly improves the time resolution of the NEXAFS (Near Edge X-Ray Absorption Fine Structure) measurements, allowing to follow under *in situ* conditions different dynamic

processes (e.g. chemical reactions) (Castan-Guerrero *et al.*, 2018). In this work, according to (Stöhr, 1992), we will use the term NEXAFS for soft X-ray absorption spectra (with an energy edge lower than 2 keV) while the name XANES (X-Ray Absorption Near Edge Structure) will be used to indicate those absorption spectra referring to hard X-rays.

Although several software packages have been developed for the analysis of hard-XAS data (e.g. GNXAS (Filipponi & DiCicco, 1995; Hatada *et al.*, 2016), ATHENA (Ravel & Newville, 2005), VIPER (Klementev, 2001), EDAXAFS (Kuzmin, 1995), SIXPACK (Webb, 2005) ...), only a few of them have been specifically designed for the data treatment of soft X-ray absorption spectra such as QANT (Gann *et al.*, 2016), Blueprint XAS (Delgado-Jaime *et al.*, 2010) or KKCalc (Watts, 2014). The critical features necessary for accurate and efficient treatment of NEXAFS data are a user-friendly interface, a quick and straightforward installation of the program on any machine, and a versatile range of functions covering the whole data treatment, from the subtraction of the background until the fit of the spectrum. THORONDOR aims to be a software for the analysis of multiple NEXAFS spectra, flexible enough to manage data collected both in conventional ultra-high vacuum (UHV) measurements and during more challenging experiments in environmental conditions. Equipped with an intuitive graphical user interface (GUI), this program, developed in Python, allows a fast data treatment and the visualization of several spectral profiles collected under different working conditions, ranging from UHV to ambient pressure atmosphere. Similarly to PyFitIt (Martini *et al.*, 2020), one of its strengths stands in the possibility to quickly perform the conventional XAS data-handling procedures, such as the spectral background subtraction and normalization, using an approach based on sliders and cursors. A peak-fitting toolbox characterized by a high variety of peak functions and ionizations step potentials is also included for in-depth studies. Herein, it is worth noting that users can exploit different minimizations algorithms to perform the peak fitting of a defined NEXAFS spectrum and evaluate, using different statistical criteria, the quality of the chosen model and the uncertainties associated to the parameters retrieved by the fit. THORONDOR has been designed principally for the analysis of TEY measurements. However, its multiple functions can also be applied for spectra collected using alternative detection modes such as Fluorescence Yield (FY).

The discussion that we propose in this article is organised as follow: after a description of the software design, we discuss how to properly handle and correct the experimental spectra in order to obtain a set of reliable and comparable data. Then, we focus on the description of the NEXAFS peak-fit toolbox and on the variety of fitting options that it provides to the user.

THORONDOR is freely distributed and can be downloaded at the following page together with more information and practical examples about its usage: <https://pypi.org/project/THORONDOR/>.

2. Structure of the Software

THORONDOR is based on two Python objects: the classes *Dataset* and *GUI*. During the initialisation procedure, a new instance of the class *GUI*, containing only temporary information, is generated.

Here, the user can provide several datasets as input to the *GUI*, as long as they focus on the same absorption edge.

The term “dataset” herein refers to the n-columns contained in a single experimental data-file, saved directly from the beamline with a minimum of two columns: the incoming photon energy, and the corresponding NEXAFS intensity. The remaining columns can contain supplementary data, such as the intensity of the incoming beam or the NEXAFS spectrum of a reference compound. At the moment, despite an important effort coming from several scientists, that consists in defining a common data exchange and archival format for X-ray experiments named NeXus-NXxas (Konnecke *et al.*, 2015), for the soft X-rays absorption measurements, there is not a well-established conventional protocol describing how an output file containing raw data should be properly formatted and designed. The number of columns characterizing a dataset thus varies depending on the beamline where the measurements are taken.

If the datasets do not possess the same exact energy range and/or number of points, all the contained spectra will automatically be interpolated on the common energy range, with a step fixed by the user.

Once that one or more datasets have been selected, a new instance of the class *Dataset*, having as its first attribute the raw data, is created for each of them, see **Figure 1**. If a logbook was compiled during the experiment and saved in an *.xlsx* format (common excel file), it can be imported in the program too. Specific experimental parameters, such as the temperature, can then be extracted from it, saved as classes attributes and used by the program. This method drastically simplifies the data analysis procedure that every scientist needs to follow after an experiment, allowing to rapidly visualize and manipulate several datasets together. The Pandas package (McKinney, 2010) is employed to transform any common format of data into a *DataFrame*: a Python object that allows a quick manipulation and visualisation of the data as array (provided by the NumPy package (Oliphant, 2006)).

It is worth noting that each new variable, parameter or model that is specific to one dataset, will be automatically saved as an attribute of the associated class. Hence, the user can always come back to resume his work, or to alternate between different datasets without losing his progress.

The THORONDOR interface is based on the Jupyter widgets package (Perez, 2007). The displayed GUI window is divided in multiple tabs. Each of them is built exploiting the *ipywidgets.HBox* and *ipywidgets.VBox* objects, containing several widgets. The instance methods of the *GUI* class are used to perform the entire data analysis. They are controlled interactively by the *ipywidgets.interact* and displayed. The result is a user-friendly interface, allowing a quick data visualisation, analysis and fitting in a Jupyter notebook environment. Each function can also be used outside the GUI for users that

possess a deeper knowledge of Python and of the class-objects functionalities. Finally, a documentation tab is provided in the GUI along with extra information reported in the online repository.

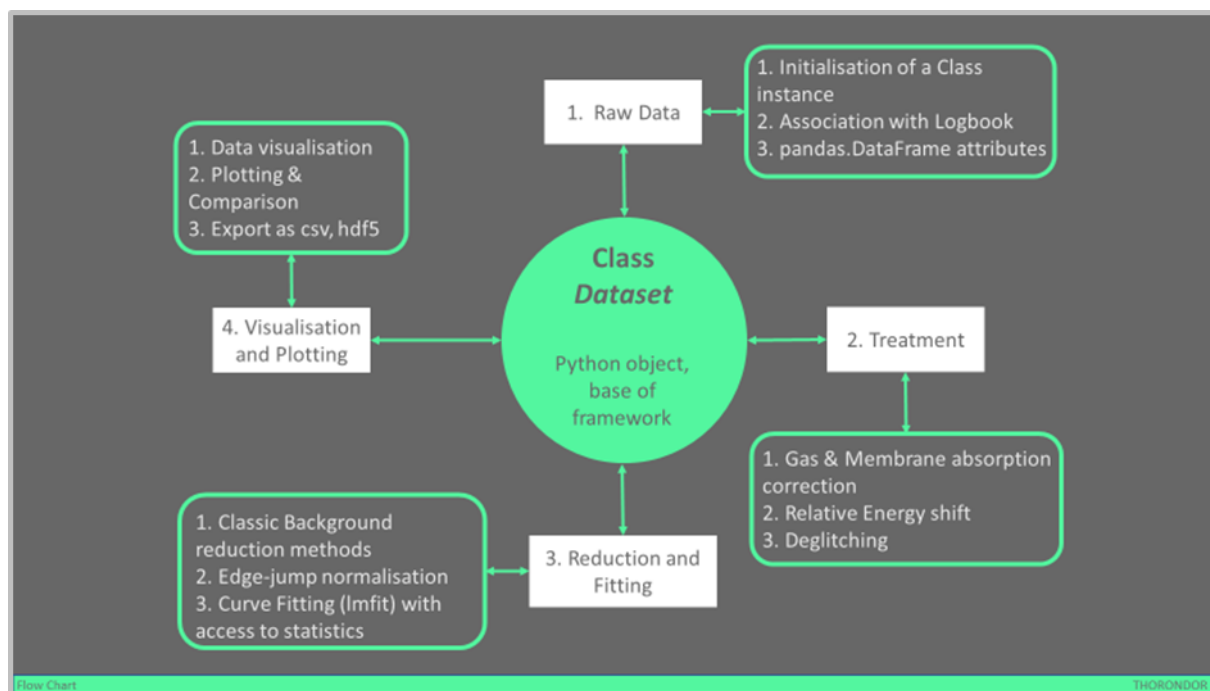


Figure 1: Flowchart of THORONDOR. A Python graphical user interface (GUI) is provided to help the user for each step of the analysis

2.1. Importing and handling raw data

The experimental data files, in *.txt* or *.dat* format, directly retrieved from the beamline, must be located inside a data folder, in the same directory as the Jupyter notebook working file, where the THORONDOR package is imported. It is supposed that the experimental files are stored in the same data folder and refer to the same energy edge. The spectral profiles coming from different experiments and belonging to different datasets can be processed only in the condition that they refer to the same absorbing element and that they share the same file architecture. As introduced in **section 2**, the raw data files can be accompanied by a logbook from which the user can extract, through a filtering method provided by THORONDOR, specific experimental information associated to each dataset, such as the data collection temperature or the composition of the gas feed. These working parameters play a fundamental role in the gas X-ray absorbance correction (see **section 2.2.2**) and in the analysis of the XAS features.

To initialize the data treatment, the user needs to provide a name for each column of every dataset contained in the working directory. Each spectrum recorded during the experiment is imported inside a *pandas.Dataframes* object under a specific column. This operation is performed using practical dropdown-widgets. Once that all the columns of a dataset have been re-named, the same nomenclature

is applied directly to all the other columns of the remaining files. It is worth noting that THORONDOR requires that at least two columns for each dataset correspond to two specific channels: the photon energy (E), and the NEXAFS intensity (μ). The latter can be computed as the ratio of the intensity of the signal coming from the sample (I_s) over the incident flux beam intensity (I_0), see **Figure 2**. The nature of I_0 and I_s depends, clearly, on the kind of measurement. In case of a TEY experiment, they consist of a current signal on the picoampere range (Castan-Guerrero *et al.*, 2018). This procedure (i.e. recording the beam intensity before the incidence on the sample) is due to the non-constant intensity of the beam in the spectrum energy range (due to the shape of the harmonic of the undulator and the transmission of the beamline optics (Stöhr, 1992)), moreover the beam in the ring can present variation in time (e.g. due to the top-up filling mode of the modern synchrotrons). Thus, the division of the absorption signal, coming from the sample, by the beam intensity, measured typically on a fine wire mesh of some noble metal, removes those artifacts from the μ shape and has become very popular among the beamline's experimental stations. In addition, if present as part of the experimental data file, the user may also specify a reference column useful for energy-alignment purposes (see section 2.2.1) and a column containing the experimental uncertainties associated to the measurement, which can be used during the peak fitting routine. It is worth noting that sometimes the flux monitor mesh can be contaminated by some elements, which are present in the sample under study too. This problem is usually addressed by normalising μ for the quantity μ_{ref} obtained as the ratio among the NEXAFS signal of a reference sample free of that target element I_{ref} for the intensity of the beam collected on the mesh I_0^{ref} : $\mu_{\text{ref}} = I_{\text{ref}}/I_0^{\text{ref}}$. This approach, named as *stable monitor method* (Watts *et al.*, 2006), is realised in THORONDOR selecting the so-called check box after the creation of the working datasets. Once that this option is activated, the user can declare which columns of the dataset (i.e. I_{ref} and I_0^{ref}) can be considered to evaluate the μ_{ref} spectrum. Afterwards the new normalised spectrum $\mu_s = \mu/\mu_{\text{ref}}$ is added to the dataframe and can undergo towards further corrections.

Initialize View Data Treatment Reduce Dataset Fit Data Plot Logbook Readme

Datafolder: ☒ Fix the name of the folder.

☒ Create/check subdirectories for the program.

Data type: Column delimiter type: Decimal delimiter type:

☐ Initial and final markers Initial Marker: Final Marker:

☐ Delete all data and reset work ! ☒ Start working !

We now start to manipulate the data.
First, rename each column and select the one we want to use.

Energy_240120_003	Is (A)_1_240120_003	Im (A)_1_240120_003	Is/Im (#)_1_240120_003	Keithley Source (A)_2_240120_003
0	815.0362	1.716600e-10	5.323630e-11	3.224492
1	814.9000	1.713744e-10	5.323555e-11	3.219172
2	814.8001	1.712643e-10	5.325696e-11	3.215811
3	814.7000	1.710960e-10	5.327742e-11	3.211417
4	814.6000	1.707806e-10	5.329397e-11	3.204501

Column: New name for this column:

This is the renamed data.

Energy	Is	I0	μ	Reference
0	775.0000	1.054999e-10	5.451449e-11	1.935263
1	775.1000	1.055966e-10	5.454800e-11	1.935847
2	775.1999	1.056825e-10	5.455501e-11	1.937173
3	775.3001	1.057797e-10	5.456408e-11	1.938633
4	775.4000	1.058620e-10	5.459794e-11	1.938938

Step: ☒ Fix step

All data files have also been corrected for the negative values of the energy and for the flipping of values.

Figure 2: The *pandas.DataFrame* object allows the quick visualisation and treatment of the dataset. Each spectrum of a dataset is recorded on the same energy range and is represented as a column in the dataframe. Here the first table shows the raw data read from the dataset referring to the first scan, while the second one reports the dataset columns selected by the user. The column μ contains here the ratio of I_s over I_0 , resulting from the *first normalization* procedure.

In THORONDOR, the signals coming from channel I_s are firstly normalized by I_0 , if such a procedure has not been performed beforehand, to produce μ . This procedure is called here *first normalization* and the related spectral intensities will be indicated in the text as μ . At the end of this scaling process, each dataframe will possess an extra column containing the first normalized signal μ . The description of the signal background subtraction followed by a further data normalization is provided in **section 2.2.4**. Finally, the plotting window tool of THORONDOR allows the user to graphically represent the information contained in each *dataframe*. Each NEXAFS spectrum can be plotted individually or together with the other signals collected during an experiment simultaneously. Herein, in order to gain a better visualization, the colour of each spectrum can be personalized by the user together with the energy range of plotting. A sketch of the program window is showed in **Figure 3**.

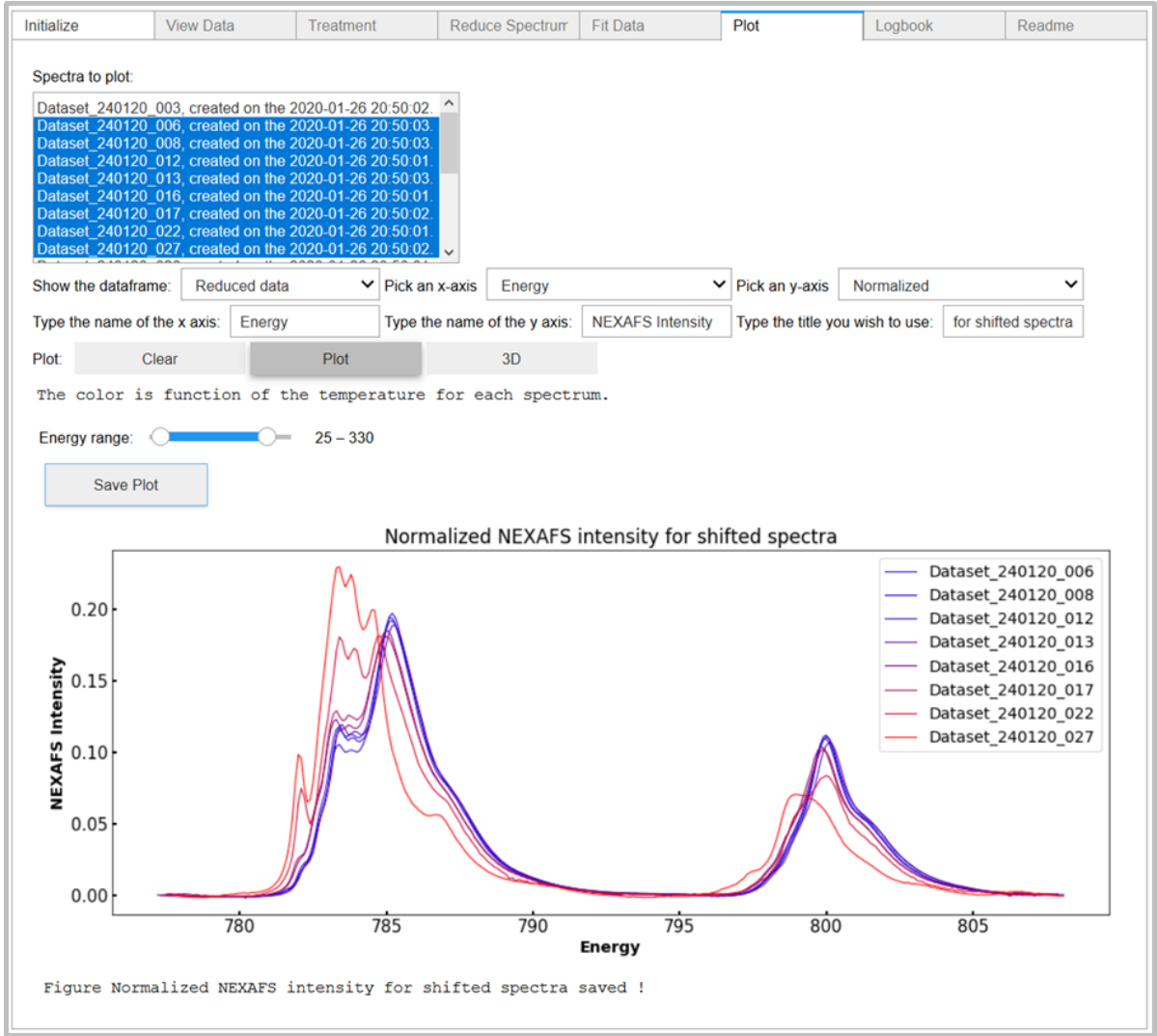


Figure 3: A sketch of the THORONDOR GUI. It is possible to display it in both Jupyter notebook and Jupyter-lab under proper builds.

2.2. Data treatment

In general, an acquired NEXAFS scan requires some corrections in order to be converted from raw data to an interpretable absorption spectrum. These spectral modifications, in THORONDOR, can be realised in four steps. These consist in: (i) the alignment of the measured spectrum to a determined reference and its subsequent calibration; (ii) the removal of eventual glitches affecting the experimental datum; (iii) the membrane and gas transmittance correction; (iv) the spectral background subtraction and *second normalization*. In the following sections, each of these steps and their implementation in the software will be described in detail.

2.2.1.Data energy alignment

It is quite common that monochromators do not retain a perfect energy calibration over the course of multiple measurements. It follows that in some cases there could be some drift or jump effects in energy within a range of a few electronvolts (Calvin, 2013). THORONDOR offers the possibility to align all datasets with respect to a common spectral feature.

If along each scan, a reference spectrum of a well-known compound (containing the same selected absorbing element) is collected simultaneously with the sample measurement, it can be used for the energy alignment procedure. The reference spectrum must be imported during the data-importing step as described in **section 2.1**. Afterwards, the user, by means of a cursor, can select the position of the same spectral feature for each reference spectrum per dataset. This yields to a list containing the position of the same feature, perchance slightly shifted, for each dataset.

Once this step is completed all the references will be shifted in energy of a quantity equal to the difference among their features and the one of the selected reference. The shifts in energy accompanying each aligned reference are automatically exported to each spectrum of every dataset, realizing, in this way, their alignment. Finally, it may happen that the reference spectrum is not acquired during the measurement. In this case, the user can align the NEXAFS spectra over a feature belonging to the I_s or μ channel.

2.2.2.Treating the effect of the window and gas X-ray absorption

Under UHV condition, it is possible to measure the photon flux I_0 impinging on the sample surface. This can be realized, for example, by measuring the TEY from a highly transparent metal grid intercepting a fraction of the incoming beam, localized, typically, before the entrance of the experimental chamber (Castan-Guerrero *et al.*, 2018). In case of ambient pressure measurements, this important part of the XAS acquisition in UHV cannot be done because of the presence of both the cell membrane and gas layer, which act as photon absorbers. However, considering these limitations, the photon flux hitting the sample I_0^{eff} can be estimated from a standard I_0 measurement before the entrance in the reaction volume and the window and gas slabs transmittances, as follow:

$$I_0^{\text{eff}} = I_0 \exp [-(k_w l_w + k_g l_g)] \quad (1)$$

Where k_w and l_w together with k_g and l_g are respectively the X-ray attenuation lengths and thickness of the membrane and of the gas. The attenuation length for an element in a given material (in the solid or gas state) is calculated as the product of the atomic density ρ_a by the atomic photo-absorption cross section σ^{abs} given by:

$$\sigma^{\text{abs}}(E) = 2r_0\lambda f_{\text{im}} \quad (2)$$

Where r_0 is the classical electron radius, λ is the X-ray wavelength and f_{im} is the imaginary part of the atomic scattering factor of the element under analysis (Henke *et al.*, 1993).

In THORONDOR, the attenuation length for the membrane refers to the Si_3N_4 compound and has been taken from the tabulated value in (Henke *et al.*, 1993). The only free parameter that, in this case, can be managed by the user is the window thickness l_w (in μm). Regarding the X-rays absorption phenomena due to the gases inside the cell, the user can easily calculate the transmittance factor for any gas mixture with THORONDOR, see **Figure 4**. In particular, given the working pressure p (in Pa) and the temperature T (in K) of one molecular component of a N-gas mixture, the related k_g term used in (1) is derived, using the following formula:

$$k_g = \sum_{j=1}^N \frac{h_j p \sigma^{\text{abs}}}{k_B T} \quad (3)$$

Where h_j is the stoichiometric index of the j^{th} element composing the molecule, while k_B is the Boltzmann constant. Once recovered, the X-ray transmittances for each gas component are multiplied by their percentual volume fraction, their final product is then equal to the total gas-mixture transmittance. It is worth noting that the described correction is not suitable if the measurement is performed at the energy edge of the elements constituting the gas phase present in the cell.

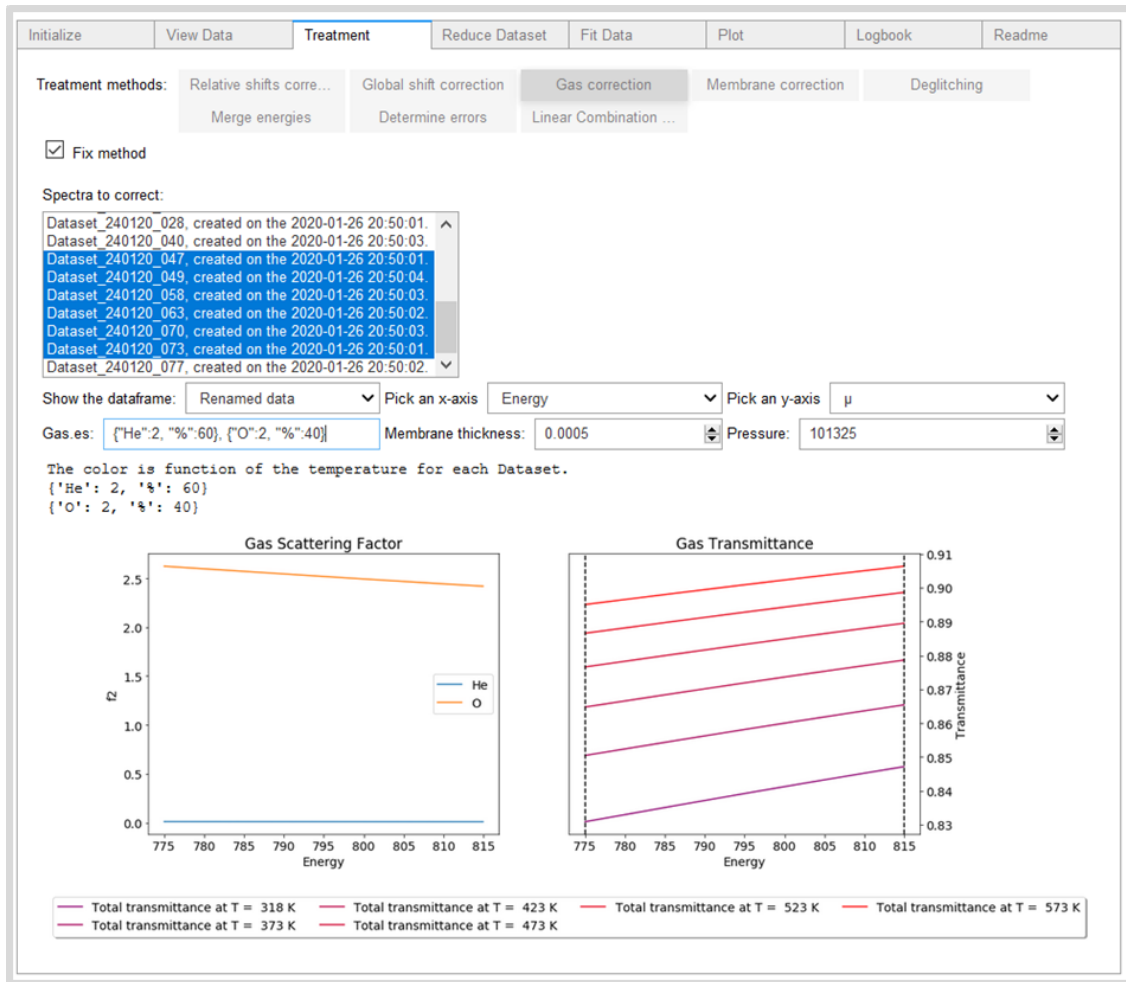


Figure 4: Plot of the gas transmittances calculated for four spectra as a function of the composition (60% He and 40% O₂) and of the temperature (showed in K for each scan in the box on the bottom part of the graph). The dashed vertical lines indicate the working energy range where the signal has been acquired (in this case within 775 eV and 815 eV).

2.2.3. Deglitching

At certain orientations, the diffraction peak being utilized by the monochromator can interfere with multiple reflections associated with another set of crystal planes (Calvin, 2013), resulting in a glitch in I_0 . Thermal (especially at high temperatures) and electrical noise can also cause some spikes in the I_s signal. The presence of glitches can distort some fundamental procedures in the program such as the background subtraction and the spectral normalization (Calvin, 2013). In THORONDOR, it is possible to select, through a single slider, the energy region surrounding a glitch and to replace it with a set of points obtained using a spline interpolating function (linear, quadratic and cubic). This curve is generated considering a user-defined number of points, situated before and after the glitch, as showed in **Figure 5**.



Figure 5: Picture of the deglitching module of THORONDOR. Moving the energy slider, it is possible to select a spectral region surrounding the glitch. Through the Deglitch button, these points will be replaced by values extrapolated by a user defined interpolating function (linear, quadratic or cubic).

2.2.4. Background subtraction and second normalization

The background removal procedure for XAS with hard X-rays, in transmission mode (excluding phenomena of self-absorption), is well established and relatively easy. It aims to subtract a pre-edge background contribution μ_b , that is usually approximated by a spline function represented by a Victoreen polynomial curve $p(E; a, b) = aE^{-3} + bE^{-4}$, whose coefficients (a, b) are obtained via least squares methods (Klementev, 2001). Afterwards, the XAS normalization is performed employing the scaling for the edge-step defined by the following formula:

$$\mu_N(E) = \frac{\mu(E) - \mu_b(E)}{\Delta\mu_0} \quad (4)$$

Where $\mu(E)$ is the raw XANES spectrum, while the normalization constant $\Delta\mu_0$, showed in (4), is the edge-step parameter. This last term is computed as the difference between the pre-edge and post-edge curves (approximated with a spline too), at the absorption edge energy E_0 . This energy value is usually identified taking the maximum of the first derivative of the XANES spectrum.

The application of the procedure to a NEXAFS spectrum may be problematic in some cases. A limitation of this method can be found when dealing with a spectrum that possess a low ionization

potential edge or when two edges are situated at close distances from each other, therefore limiting the pre and post-edge energy ranges used to define the spline functions, see **Figure 6**. The estimation of the edge jump will contain, in this case, a larger uncertainty.

Further problems can emerge also if the spectra have been acquired outside the UHV conditions. In particular, the NEXAFS background can increase with the gas absorption of the X-ray beam and, at the same time, some signal features can be distorted if the gas concentration quickly changes during a spectrum acquisition (Castan-Guerrero *et al.*, 2018).

Beside these particular cases, the problem is caused by the electron detection mode so popular in the soft X-ray range. In fact, for one absorbed photon, n electrons are generated, a number depending from a high number of parameters that are not always constant in the energy range of the spectrum. This effect give rise to slopes that are superimposed to the NEXAFS spectrum (often called background) and that alter the shape of the spectrum thus making difficult the extrapolation of the meaningful information.

THORONDOR offers five different techniques which can be exploited to subtract the NEXAFS background. In the GUI, these methods are indicated as: *Splines*, *Single spline*, *Polynomial curves*, *Asymmetric Least Squares* and *Chebyshev polynomials*. The first method, *Splines*, has been described earlier for hard X-rays. It is recommended only for those spectra which have been acquired in ultra-high vacuum (UHV) or referring to samples with a high concentration of the absorber element. The *Single spline* method is the fastest to execute and allows a quick visualization of the data quality during an experiment. The last three approaches are suitable for NEXAFS data characterized by a non-linear variation of the background and by an extremely small edge jump, similar to those reported in **Figure 6**. Each of these techniques is described in detail from section **2.2.4.1** to **2.2.4.5**

In THORONDOR, for each method, the parameters regulating the generation of the background curves are completely accessible to the user through sliders. In particular, the program allows, for a user-defined energy range, the simultaneous visualization of the original (untreated) spectrum and the background subtracted spectrum on two separated graphic windows. Once defined for a spectrum (e.g. μ) in a first dataset, the same background subtraction parameters can be applied to the other spectra for all the acquired datasets. This is an important feature of THORONDOR that allows the user to define a set of parameters on one dataset, and to then, if satisfactory, to use the same parameters on the other datasets. Thereby quickly correcting the background for all datasets and allowing a quick visualisation of the corrected data.

In case of a NEXAFS signal treated using the *Splines* method, the *second normalization* procedure is realised using equation (4). For the other cases, the intensity of each NEXAFS point is divided by the total area under the background subtracted curve.

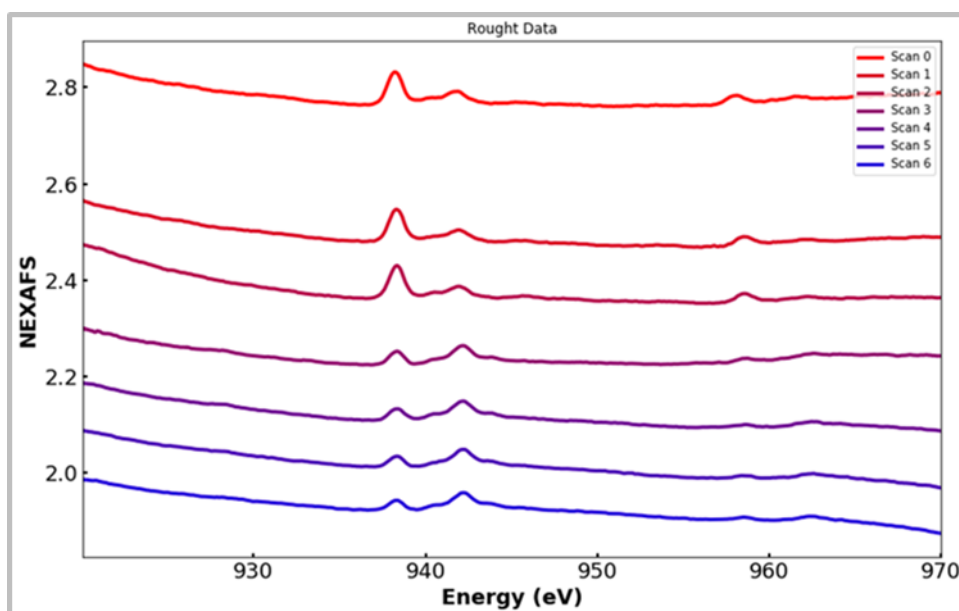


Figure 6: Plot of seven NEXAFS (μ) scans referring to the Cu L_2 and L_3 edges acquired during the cooling ramp (from 135 °C to 100 °C) in presence of CO for a Cu-exchanged CHA zeolite (Cu/Al=0.5, Si/Al=15; Cu 2.6 wt%: typical example of diluted absorbing element). It is evident from the graph that the classical background subtraction and normalization procedure typical of the hard-XAS here cannot be applied because of low edges absorption jump and due to non-linear background.

2.2.4.1. Splines method

The first step of this technique consists in the identification of the absorption energy edge (E_0) for the spectrum under analysis. This is done, in the program, by calculating the first order derivative of the NEXAFS spectrum and by taking the energy value of its maximum. The selection of the maximum of the derivative is done automatically by the program. However, the user has the possibility, through a cursor, to select a specific point of the derivative curve and to save the related energy value as E_0 . Once that the value of the edge energy position has been defined, the user can start to manipulate two sliders controlling the number of energy points situated, respectively, in the pre-edge and post-edge part of the NEXAFS spectrum. These two set of points are used to define the pre-edge and post-edge spline functions which are subsequently employed to remove the background and normalize the spectrum in accordance to equation (4). THORONDOR offers also different kind of interpolating functions which can be used instead of the classical splines introduced in 2.2.4. These include linear, quadratic and cubic polynomial models, which exploit the *numpy.polyfit* method (Oliphant, 2006). An example where this method is applied with success is showed in **Figure 7**.

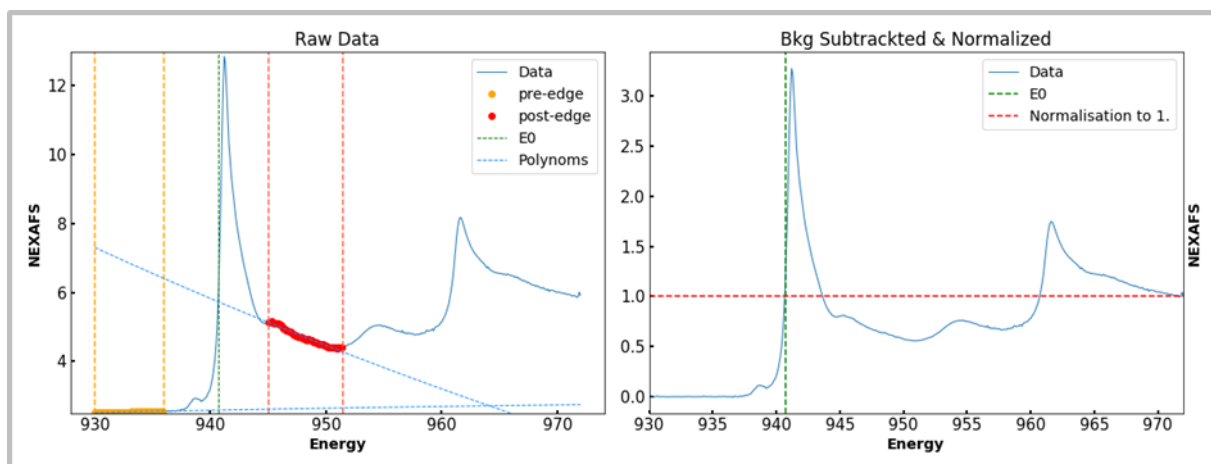


Figure 7: Cu L_3 and L_2 edge NEXAFS spectra for Cu_2O (representative example of highly concentrated absorbing element), before (left panel) and after (right panel) the background subtraction and normalization provided by the splines method. The yellow and red vertical lines and the colour-related points indicate the selected pre-edge and post-edge regions, respectively. The green dashed line denotes in both graphs the position of the energy position of the absorption edge (E_0).

2.2.4.2. Single Spline method

This method can be used as an alternative normalization procedure for a NEXAFS spectrum whose background has been subtracted with the same kind of interpolating curves (splines or polynomials) employed in the Splines method described in section 2.2.4.1. Through a single slider, the user can select the number of points situated in the pre-edge of the NEXAFS spectrum. Once this step is completed, this range of points is fitted by a spline or a polynomial function, which is subsequently subtracted from the raw NEXAFS spectrum. Contrary to the *classic* Splines method, which foresees the edge-step normalization, this procedure is realised by scaling the background subtracted NEXAFS spectrum to the magnitude of a point in the curve (e.g. the maximum peak intensity of the NEXAFS white-line or a point corresponding to the maximum value of the energy range (Qayyum *et al.*, 2013)), which is selected through the usage of a proper slider. A demonstrative representation of this approach is showed in **Figure 8**.

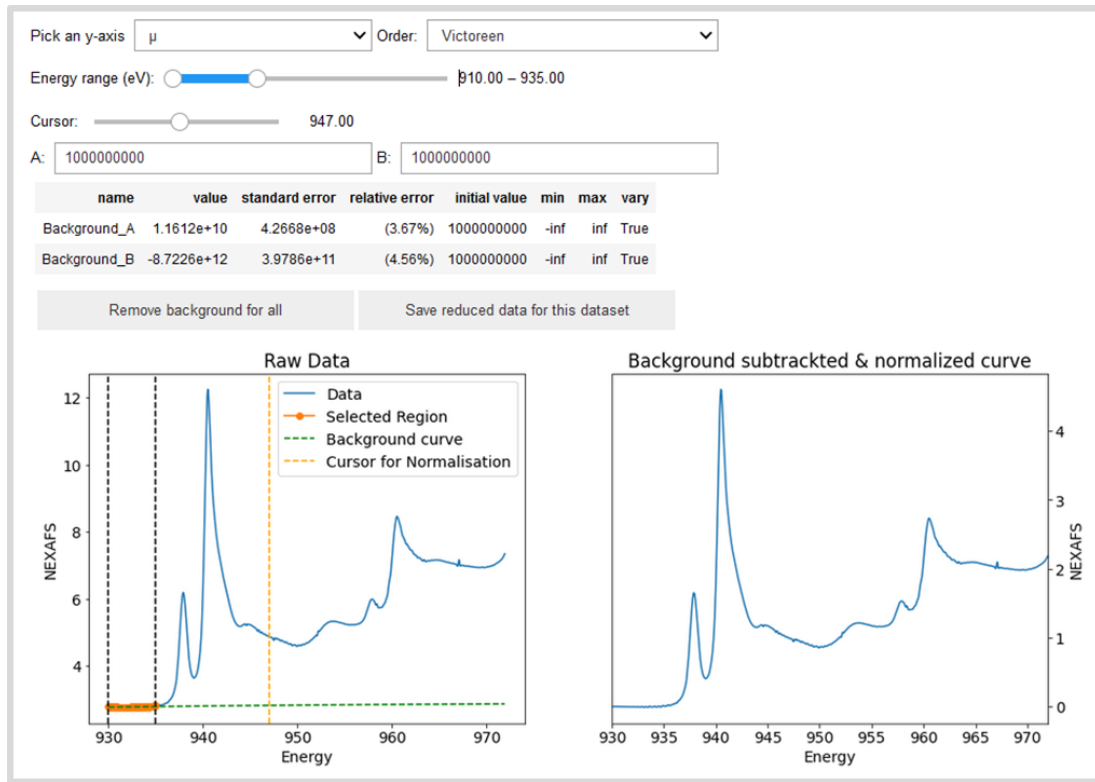


Figure 8: Sketch of the THORONDOR single spline method tab window. The orange points enclosed within the two dashed black vertical lines represent the NEXAFS values in the pre-edge employed to generate the green spline curve, which is then subtracted from the experimental spectrum. The vertical orange dashed curve identifies a NEXAFS point whose intensity is used to scale the entire NEXAFS spectrum.

2.2.4.3. Polynomial curves method

Given an experimental spectrum, a background curve is generated based on a determined number of points $\mu(E_i)$ belonging to the NEXAFS signal. The amounts of points and position in energy are user defined. Through sliders, the user can distribute them along the entire spectrum selecting specific energy positions which are not characterized by real spectral features but uniquely by the signal background (e.g. some region of the spectrum without any peak), see **Figure 9**. Once that this step is completed, the related background function, consisting in a third order spline, is generated, using the *splrep* method of the SciPy package (Virtanen, 2020), and directly subtracted from the raw data.

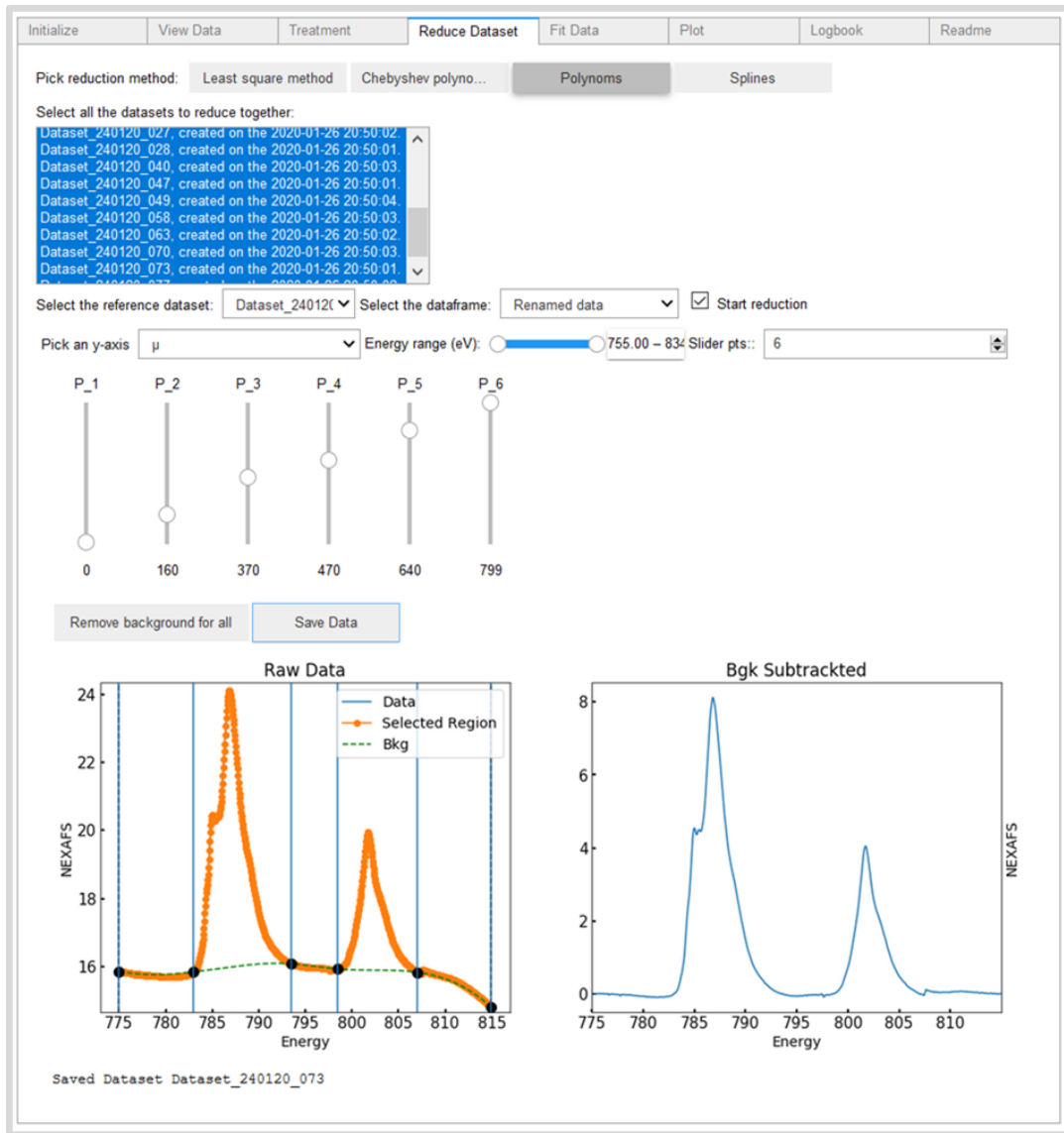


Figure 9: Application of the polynomial curves method to remove the background from a representative NEXAFS spectrum at Co L-edge (orange points, left panel) containing both the L₂ and L₃ edges. After having selected the working energy range and the number of spectral points needed to generate the background function, the user can move them along the spectral profile through sliders while simultaneously observing their effect on the background subtracted spectrum (blue curve, right panel).

2.2.4.4. Asymmetric Least Squares method

Among all the approaches, the Asymmetric Least Squares method has proven to be the fastest and most accurate. This baseline subtraction approach was introduced by Eilers and Boelens and it has been extensively used in the field of Raman spectroscopy (Baek *et al.*, 2015; Eilers, 2003). It exploits an asymmetric least squares (AsLS) method. The method aims at fitting a smooth background f to an experimental spectrum $\mu(E)$. To do so, it is necessary to minimize the following objective function:

$$\operatorname{argmin}_f \left\{ \sum_{i=1}^N w_i (\mu(E_i) - f_i) + \lambda \sum_{i=1}^N (\Delta^2 f_i)^2 \right\} \quad (5)$$

The first term of equation (5) expresses the goodness of the data fitting while the second one is related to the smoothness of f . Herein $\mu(E_i)$ and f_i are respectively the i^{th} value of the experimental NEXAFS spectrum (μ having N values) and the smoothed function f evaluated at the i^{th} energy point. The $\Delta^2 f_i$ term is a difference operator defined as: $\Delta^2 f_i = (f_i - f_{i-1}) - (f_{i-1} - f_{i-2}) = f_i - 2f_{i-1} + f_{i-2}$, λ is a regularization parameter while w_i represents a set of weights chosen asymmetrically: $w_i = p$ if $\mu(E_i) > f_i$ and $w_i = 1 - p$ otherwise. In THORONDOR, the user can have direct access to λ and p and consequently move them in the recommended ranges within $10^7 - 10^9$ for λ and $0.001 - 0.1$ for p (Baek *et al.*, 2015). Once that the parameters have been chosen, the background function is automatically generated and subtracted to the experimental spectrum. The THORONDOR tab window designed for this approach is reported in **Figure 10**.

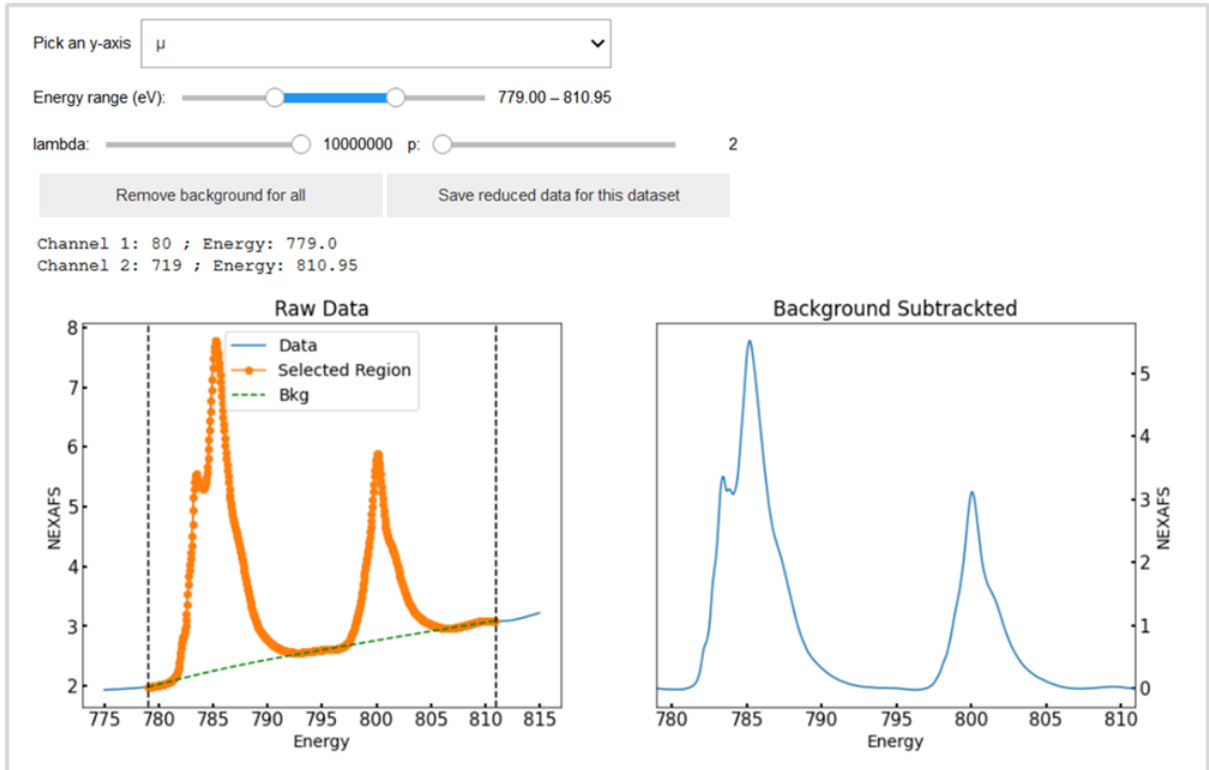


Figure 10: Application of the asymmetric least squares method to remove the background from a representative region of a NEXAFS spectrum, corresponding to the Co L-edge (orange points, left panel), containing both the L_2 and L_3 edges. The parameters λ and p , controlled by sliders, are the ones appearing in equation (5) and modify directly the shape of the background subtracting curve.

2.2.4.5. Chebyshev polynomials method

This method has been already applied with success to powder diffractograms (Simonne, 2019). The first kind Chebyshev polynomials T_i can be derived using the following equation:

$$f(E, \mathbf{a}) = \sum_{i=0}^N a_i T_i(E) + \varepsilon \quad (6)$$

The term \mathbf{a} consists in a vector containing a set of coefficients where a_i is the $N + 1$ coefficient determined by a weighed least square regression.

The degree N of the equation must be determined empirically, the weights, optional, can simply be taken as the square of the variance of the counting statistics to prevent the function from fitting the spectral peaks. The background $f(E, \mathbf{a})$ is then assimilated as a summation of Chebyshev polynomials where each of them fits a small area of the spectrum, see **Figure 11**. The number of polynomials must be high enough in order to take account for the baseline and avoid the fitting of the existing curve. This method usually shows problems with peaks with a large FWHM where the polynomials tend unfortunately to fit the peaks. On the contrary, the method is very effective for peaks possessing a small FWHM.

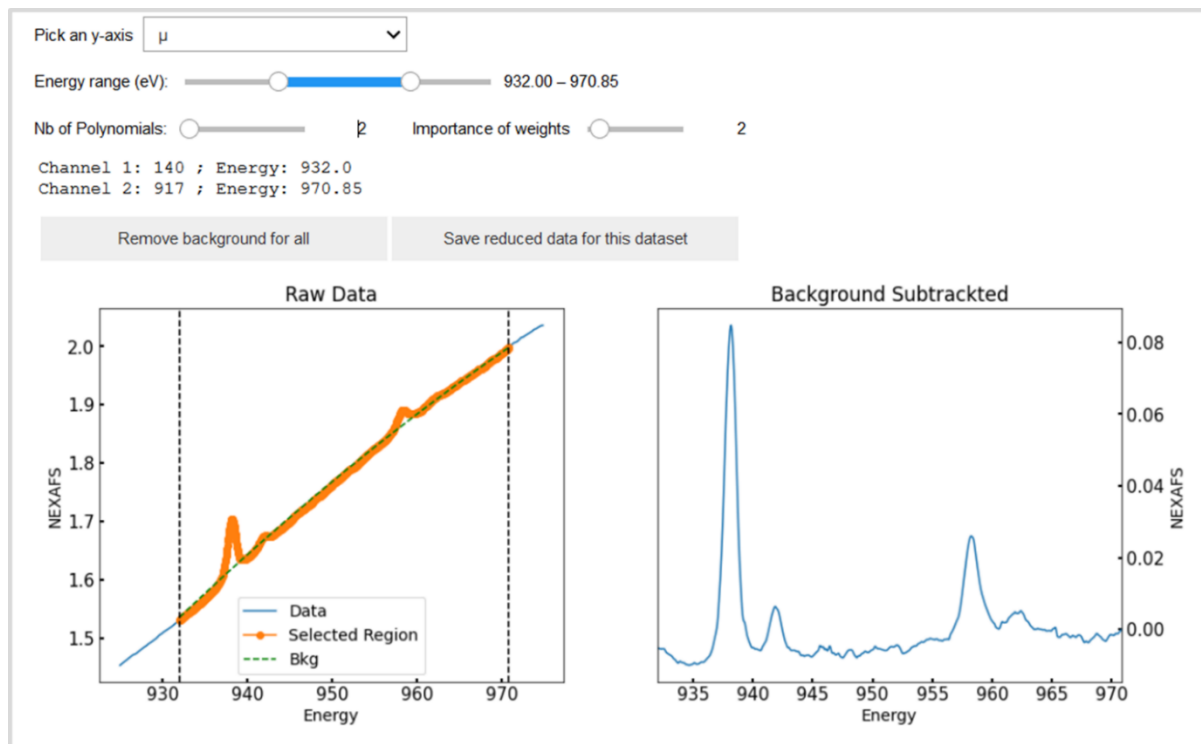


Figure 11: Application of the Chebyshev polynomials method to remove the background from a representative region of a NEXAFS spectrum, corresponding to the Cu L-edge (orange points, left panel), containing both the L_2 and L_3 edges. The degree N of the polynomials and the importance of weights can be changed by sliders and control directly the shape of the background curve computed *via* the NumPy classmethod `Chebyshev.fit` function.

3. Peak fitting

Once that the data treatment procedure (described in **section 2.2**) is completed, a NEXAFS spectrum can be further processed using the THORONDOR peak-fitting toolbox.

In general, a NEXAFS spectrum is always characterized by resonances corresponding to different transitions from an occupied core state to an unfilled final state (Gann *et al.*, 2016). These resonances can be usually modelled as peak shapes, properly reproduced by Lorentzian peak-functions (de Groot, 2005; Henderson *et al.*, 2014; Stöhr, 1992; Watts *et al.*, 2006). The procedure of peak decomposition becomes extremely important when someone wants to decompose a NEXAFS spectrum into a set of peaks where each of them can be assigned to an existing and physically reasonable electronic transition. Finally, spectral energy shifts for a set of scans can be recovered from the fitting procedure too. They correspond to inflection points in the absorption edge step function (i.e. the maximum of their first derivatives). The evaluation of these quantities is extremely important because they properly indicate the presence of reduction or oxidation phenomena involving the absorber atoms in the system under study.

THORONDOR offers a large class of peak functions including Gaussian, Lorentzian, Voigt and pseudo-Voigt profiles. The signal absorption edge step can be properly modelled using an arc-tangent function (Poe *et al.*, 2004) as well as an error function, which have been proven to be suitable for this usage too (Henderson *et al.*, 2014; Outka & Stöhr, 1988). In general, the user should pick a step-function according to his knowledge prior to the fitting, since it has been shown that the width of the error function is related to the instrumental resolution (Outka & Stöhr, 1988), whereas the width of the arc-tangent is connected with the life-time of the excited state. The step localization depends on the quality of the spectrum, usually several eV below the core level ionization energy (Outka & Stöhr, 1988). Sometimes, the background in the pre-edge can slightly differ from the step function due to features linked to transition to the bound states in the system (de Groot, 2005). In THORONDOR, if one wishes to focus on that energy range, it is possible to use splines of different order to fit the baseline for those energy values and then pass to fit and normalize the pre-edge peaks (Wilke *et al.*, 2001).

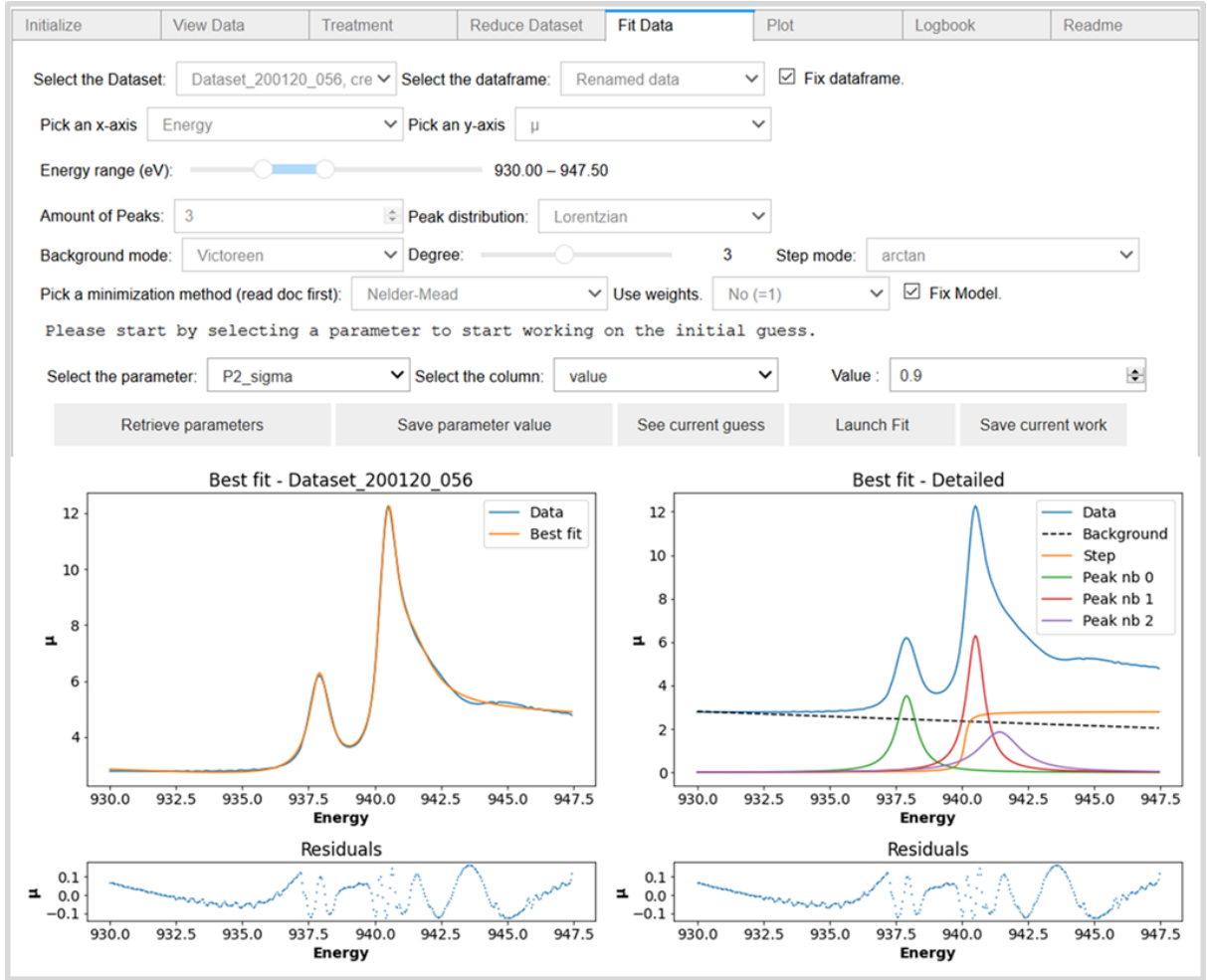


Figure 12: Screenshot of the THORONDOR peak-fitting toolbox. In the graph on the left is reported the comparison between the experimental spectrum and the best fit referring to a Cu_2O sample, while on the right are showed all the optimized profiles. The associated R-factor, quantifying the misfit among the experiment and the best fit is $R_{XS}^2(\%) = 0.15\%$.

In THORONDOR, the parameters associated with the peak and step profiles (i.e. the number of peaks and their energy position, their FWHM, the peak function amplitudes, the number of step functions and their slopes ...) are defined by the user *via* cursors and text-boxes, see **Figure 12**. After the definition of a fitting model, the user needs to provide an initial guess to initialise the fitting routine. The sum of all the user-defined functions with the current guess for the parameters is plotted along the experimental spectrum by clicking on the button *See current guess*. Therefore, by tuning the initial guess, the user can visualise the agreement between the experimental curve and the reconstructed one. Once that this step is performed, the user-defined parameters are employed to initialize the fitting routine.

The fitting routine is based on the minimization of a square residual objective function Ξ , defined as:

$$\Xi(\mathbf{p}) = \sum_{i=1}^N \frac{(\mu^{\text{exp}}(E_i) - \mu^{\text{theo}}(E_i, \mathbf{p}))^2}{\epsilon_i^2} \quad (7)$$

Where $\mathbf{p} = (p_1, \dots, p_M)$ is the set of M parameters characterizing the selected peak and step functions, N is the number of the energy points, $\mu^{\text{exp}}(E_i)$ and $\mu^{\text{theo}}(E_i, \mathbf{p})$ are respectively the i^{th} value of the experimental and the theoretical spectrum, while ε_i is the *uncertainty weighting* related to the i^{th} experimental point. Equation (7) assumes that the experimental signal is only affected by random Gaussian noise with standard deviation equal to ε_i around the true signal (Filipponi & DiCicco, 1995). Thanks to the use of the *lmfit* packaged (Newville, 2014), THORONDOR provides different minimizations algorithm that can be applied to minimize equation (7). In particular, the Levenberg-Marquardt algorithm (Moré, 1978) is recommended for the fitting procedure if the user decides to start the analysis with a good initial guess. Indeed, this method is quite fast and converges quickly towards a local minimum. If the fitting routine does not succeed, some additional algorithms are provided, such as the Nelder-Mead method (Nelder & Mead, 1965) which has been demonstrated to be more robust than the precedent one (Newville, 2014).

3.1. Estimating the experimental uncertainties

As it is possible to see from (7), the definition of \mathcal{E} requires the evaluation of the experimental errors ε_i . If these are not provided by the user, THORONDOR offers three different alternatives.

The first procedure has been inspired by the work by Dent et al. (Dent *et al.*, 1992) and it is employed in the GNXAS software to estimate the error associated to an experimental EXAFS spectrum (Filipponi & DiCicco, 1995). It is based on three parts: first of all, few points (from three to twenty) are selected in the spectrum around a point. Secondly, a low order polynomial (degree one, two or three) is fitted on the selected data. Third, the root mean square (rms) deviation of all the data within the selected range, from the polynomial curve, is assigned to the selected NEXAFS point. This last procedure is then repeated on several narrow intervals along the total spectrum. Finally, all the extracted rms values are interpolated with a smooth function and its inverse is used as the error term in (7).

The second method simply uses the errors from the user, imported along with the data, as uncertainty weights for equation (7).

Finally, in case the errors provided by the first method seem under- or over-estimated and if the user is unable to quantify the uncertainty on the measure, the errors can either be equalled to the inverse of the background subtracted data or to one, resulting in a non-weighted fitting routine for the latter.

3.2. Evaluation of the goodness of a fit

Mismatch between data and fit can be measured in a number of ways (Calvin, 2013). One of the common methods implemented in THORONDOR is the XAFS R-factor. According to the International XAFS Society Standard and Criteria Committed (Committee, 2000) it is defined as:

$$R_{\text{IXS}}^2(\%) = 100 \times \frac{\sum_{i=1}^N (\mu^{\text{exp}}(E_i) - \mu^{\text{theo}}(E_i, \mathbf{p}))^2}{\sum_{i=1}^N (\mu^{\text{exp}}(E_i))^2} \quad (8)$$

In the hypothesis that the S/N ratio of the data is good, the $R_{\text{IXS}}^2(\%)$ of an adequate fit can be expected to be in the order of few percent (Calvin, 2013; Committee, 2000).

Because of the presence of M parameters in the fit, the quantity $\Xi(p_1^0, \dots, p_M^0)$, where the vector $\mathbf{p}^0 = (p_1^0, \dots, p_M^0)$ is the minimum value of (7), can be interpreted by a χ_{N-M}^2 random variable. Thus, the statistical χ^2 test can be performed in THORONDOR to check if the actual value of $\Xi(p_1^0, \dots, p_M^0)$ is only due to the residual noise or otherwise it contains unexplained physical information (Filipponi & DiCicco, 1995).

3.3. Finding uncertainties in fitted parameters

In THORONDOR, the parameter uncertainties retrieved by the fitting procedure can be estimated in different ways. In general, this is done by inverting the Hessian matrix of (7) determining the related covariance matrix, whose diagonal elements are the squared parameters errors (Bunker, 2010). However, sometimes the uncertainties cannot be estimated, which generally indicates that Hessian matrix cannot be properly inverted because the fit is not actually sensitive to one of the variables that must be optimized. This can happen if a parameter is stuck at an upper or lower bound, if the variable is simply not used by the fit or if the value, for that variable, is such that it has no real influence on the fit (Newville, 2014). Moreover, as already introduced in **section 3**, the standard errors computation assume that the residuals $\text{RES}(E_i) = \mu^{\text{exp}}(E_i) - \mu^{\text{theo}}(E_i, \mathbf{p})$ follow a normal distribution with mean equal to zero, and that a map of probability distributions for pairs of parameters would be elliptical (the size of the ellipse gives the uncertainty while the eccentricity the correlation) (Bevington, 2003; Newville, 2014). The validity of the uncertainty estimation can be discussed since it ignores outliers, highly asymmetric uncertainties, or complex correlations between the estimated parameters. Nevertheless, the results that yield from this estimation are usually pretty good when it is possible to determine them, which is usually the case if one starts the algorithm with an initial guess close enough to a local minimum.

A more detailed investigation of the probability distribution of the parameters can be performed a posteriori via the *emcee* Markov Chain Monte Carlo package (Foreman-Mackey *et al.*, 2013) (version 3 or superior) by exploring the parameter space. This additional step is recommended, especially if the estimation of the covariance matrix fails, roadblocks can be present with models composed of numerous parameters and bounds or constraints. Hence, one can estimate the uncertainties and find the correlations between pairs of parameters. A corner plot can be drawn using the *corner* package (Foreman-Mackey, 2016).

As described before, in THORONDOR, confidence intervals are determined in both methods providing a clear idea of the uncertainties associated to each parameter. Overall, the fitting module of THORONDOR allows one to quickly fit specific features or entire spectra using different approaches and many degrees of freedom, without neglecting the statistical analysis of the fit quality.

4. Conclusions and perspectives

In this paper, we have presented THORONDOR, a free software designed in Python, suitable for the quick analysis of large series of NEXAFS spectra collected under UHV or during an *in situ* experiment. The program allows to correct and normalize the acquired XAS spectra using various quick techniques, directly and interactively accessible by the user via sliders and cursors. After the selection of a NEXAFS spectrum, by exploiting the THORONDOR fitting toolbox, the user can recover the energies and intensities of the most prominent absorption features together with their uncertainties. In particular, different peak functions (Gaussian, Lorentzian, Voigt ...) and absorption edge step functions (arc-tangent, error functions, ...) can be employed for this purpose.

Regarding the future development perspectives of this software, we are going to implement three new tools. i) First, we are going to make THORONDOR suitable to read and deal with the NeXus-NXxas data file format (Konnecke *et al.*, 2015), which is imposing as one of the most employed data format for the entire XAS community. In particular, the software will be able to extract, visualise and save the metadata contained in each file, which can be rich of information about the experimental conditions of the NEXAFS measurements (e.g. sample temperature, sample positions in the beamline end-station ...etc.). ii) We intend to insert in THORONDOR a section dedicated to the compositional analysis of the acquired experimental spectra. The new module will allow to perform the linear combination fit of a NEXAFS spectrum on the basis of user-defined references. Moreover, we are also considering the possibility to implement a second module realizing the spectral decomposition procedure based on the Multivariate Curve resolution-Alternating Least Squares (MCR-ALS) algorithm (Jaumot *et al.*, 2005). iii) Finally, since it is progressively becoming a standard procedure to understand the collected NEXAFS data, we are going to interface THORONDOR with the simulated spectroscopic data coming directly from different time-dependent density functional theory (TD-DFT) calculations (e.g. the Amsterdam Density Functional (Atkins *et al.*, 2013; te Velde *et al.*, 2001)) or from the atomic multiplet simulations (de Groot, 2005) (e.g. Quanty (Haverkort & Iop, 2016; Haverkort *et al.*, 2012)), which can be compared with the experimental spectra obtained after the data treatment procedure.

Funding

This work has received support from project PRIN-2017 MOSCATo (Cutting-edge X-ray methods and models for the understanding of surface site reactivity in heterogeneous catalysts and sensors).

Acknowledgements

We are grateful to E. Groppo (University of Turin), F. Tavani, P. D'Angelo (University of Rome, La Sapienza) and P. Ghigna (University of Pavia) for the several fruitful discussions about the NEXAFS data treatment procedures and for their contribution in the field of soft X-rays analysis. We thank A. A. Guda, S. A. Guda, and A. V. Soldatov (The Smart Materials Research Center, Southern Federal University) for the useful advices connected with the architecture of the THORONDOR code and S. Zafeiratos (CNRS and University of Strasbourg) for having provided us a set of samples which has also represented a useful testing ground for the program.

We are deeply indebted with Prof. C. Lamberti, an amazing mentor and a brilliant guide who, unfortunately, left us too early.

References

- Atkins, A. J., Bauer, M. & Jacob, C. R. (2013). *Phys. Chem. Chem. Phys.* **15**, 8095-8105.
- Baek, S. J., Park, A., Ahn, Y. J. & Choo, J. (2015). *Analyst* **140**, 250-257.
- Beaumont, S. K. (2020). *Phys. Chem. Chem. Phys.*
- Bevington, P. R. a. R., D. Keith (2003). *Data reduction and error analysis for the physical sciences*, 3rd ed. ed. New York, NY: McGraw-Hill.
- Blum, M., Weinhardt, L., Fuchs, O., Bar, M., Zhang, Y., Weigand, M., Krause, S., Pookpanratana, S., Hofmann, T., Yang, W., Denlinger, J. D., Umbach, E. & Heske, C. (2009). *Rev. Sci. Instrum.* **80**, 6.
- Bunker, G. (2010). *Introduction to XAFS: A Practical Guide to X-ray Absorption Fine Structure Spectroscopy*. Cambridge: Cambridge University Press.
- Calvin, S. (2013). *XAFS for Everyone*.
- Castan-Guerrero, C., Krizmancic, D., Bonanni, V., Edla, R., Deluisa, A., Salvador, F., Rossi, G., Panaccione, G. & Torelli, P. (2018). *Rev. Sci. Instrum.* **89**, 8.
- Committee, I. S. a. C. (2000).
- de Groot, F. (2005). *Coord. Chem. Rev.* **249**, 31-63.
- Delgado-Jaime, M. U., Mewis, C. P. & Kennepohl, P. (2010). *J. Synchrotr. Radiat.* **17**, 132-137.
- Dent, A. J., Stephenson, P. C. & Greaves, G. N. (1992). *Rev. Sci. Instrum.* **63**, 856-858.
- Eilers, P. H. C. (2003). *Anal. Chem.* **75**, 3631-3636.
- Escudero, C., Jiang, P., Pach, E., Borondics, F., West, M. W., Tuxen, A., Chintapalli, M., Carencio, S., Guo, J. H. & Salmeron, M. (2013). *J. Synchrotr. Radiat.* **20**, 504-508.
- Filipponi, A. & DiCicco, A. (1995). *Phys. Rev. B* **52**, 15135-15149.
- Foreman-Mackey, D. (2016). *The Journal of Open Source Software* **1**.
- Foreman-Mackey, D., Hogg, D. W., Lang, D. & Goodman, J. (2013). *Publ. Astron. Soc. Pac.* **125**, 306-312.
- Forsberg, J., Duda, L. C., Olsson, A., Schmitt, T., Andersson, J., Nordgren, J., Hedberg, J., Leygraf, C., Aastrup, T., Wallinder, D. & Guo, J. H. (2007). *Rev. Sci. Instrum.* **78**, 7.
- Fuchs, O., Maier, F., Weinhardt, L., Weigand, M., Blum, M., Zharnikov, M., Denlinger, J., Grunze, M., Heske, C. & Umbach, E. (2008). *Nucl. Instrum. Methods Phys. Res. Sect. A-Accel. Spectrom. Dect. Assoc. Equip.* **585**, 172-177.
- Gann, E., McNeill, C. R., Tadich, A., Cowie, B. C. C. & Thomsen, L. (2016). *J. Synchrotr. Radiat.* **23**, 374-380.
- Guda, A. A., Guda, S. A., Lomachenko, K. A., Soldatov, M. A., Pankin, I. A., Soldatov, A. V., Braglia, L., Bugaev, A. L., Martini, A., Signorile, M., Groppo, E., Piovano, A., Borfecchia, E. & Lamberti, C. (2019). *Catal. Today* **336**, 3-21.
- Guo, J. H. & Luo, Y. (2010). *J. Electron Spectrosc. Relat. Phenom.* **177**, 181-191.

- Hatada, K., Iesari, F., Properzi, L., Minicucci, M., Di Cicco, A. & Iop (2016). *Journal of Physics Conference Series*, Vol. 712, *16th International Conference on X-Ray Absorption Fine Structure*, Bristol: Iop Publishing Ltd.
- Havecker, M., Knop-Gericke, A. & Schedel-Niedrig, T. (1999). *Appl. Surf. Sci.* **142**, 438-442.
- Haverkort, M. W. & Iop (2016). *Journal of Physics Conference Series*, Vol. 712, *16th International Conference on X-Ray Absorption Fine Structure*, Bristol: Iop Publishing Ltd.
- Haverkort, M. W., Zwierzycki, M. & Andersen, O. K. (2012). *Phys. Rev. B* **85**, 20.
- Henderson, G. S., de Groot, F. M. F. & Moulton, B. J. A. (2014). *Reviews in Mineralogy & Geochemistry*, Vol. 78, *Spectroscopic Methods in Mineralogy and Materials Sciences*, edited by G. S. Henderson, D. R. Neuville & R. T. Downs, pp. 75-+. Chantilly: Mineralogical Soc Amer & Geochemical Soc.
- Henke, B. L., Gullikson, E. M. & Davis, J. C. (1993). *Atom. Data Nucl. Data Tables* **55**, 349-349.
- Jaumot, J., Gargallo, R., de Juan, A. & Tauler, R. (2005). *Chemometrics Intell. Lab. Syst.* **76**, 101-110.
- Klementev, K. V. (2001). *J. Phys. D-Appl. Phys.* **34**, 209-217.
- Kluyver, T. (2016). pp. 87-90. ELPUB.
- Knop-Gericke, A., Havecker, M., Neisius, T. & Schedel-Niedrig, T. (1998). *Nucl. Instrum. Methods Phys. Res. Sect. A-Accel. Spectrom. Dect. Assoc. Equip.* **406**, 311-322.
- Konnecke, M., Akeroyd, F. A., Bernstein, H. J., Brewster, A. S., Campbell, S. I., Clausen, B., Cottrell, S., Hoffmann, J. U., Jemian, P. R., Mannicke, D., Osborn, R., Peterson, P. F., Richter, T., Suzuki, J., Watts, B., Wintersberger, E. & Wuttke, J. (2015). *J. Appl. Crystallogr.* **48**, 301-305.
- Kuzmin, A. (1995). *Physica B* **208**, 175-176.
- Lassalle-Kaiser, B., Gul, S., Kern, J., Yachandra, V. K. & Yano, J. (2017). *J. Electron Spectrosc. Relat. Phenom.* **221**, 18-27.
- Martini, A., Guda, S. A., Guda, A. A., Smolentsev, G., Algasov, A., Usoltsev, O., Soldatov, M. A., Bugaev, A., Rusalev, Y., Lamberti, C. & Soldatov, A. V. (2020). *Comput. Phys. Commun.* **250**, 15.
- McKinney, W. (2010). *Proceedings of the 9th Python in Science Conference*, pp. 51 - 56. Stéfán van der Walt and Jarrod Millman
- Mino, L., Agostini, G., Borfecchia, E., Gianolio, D., Piovano, A., Gallo, E. & Lamberti, C. (2013). *J. Phys. D-Appl. Phys.* **46**, 72.
- More, J. J. (1978). *Numerical Analysis*, edited by G. A. Watson, pp. 105-116. Berlin, Heidelberg: Springer Berlin Heidelberg.
- Nelder, J. A. & Mead, R. (1965). *The Computer Journal* **7**, 308-313.
- Newville, M., Stensitzki, Till, Allen, Daniel B., & Ingargiola, Antonino. (2014). *Zenodo*.
- Oliphant, T. E. (2006). *A guide to NumPy*. Trelgol Publishing USA.
- Outka, D. A. & Stohr, J. (1988). *J. Chem. Phys.* **88**, 3539-3554.
- Perez, F. a. G., B. E. (2007). *Computing in Science Engineering* **9**, 21-27.
- Poe, B. T., Romano, C. & Henderson, G. (2004). *J. Non-Cryst. Solids* **341**, 162-169.
- Qayyum, M. F., Sarangi, R., Fujisawa, K., Stack, T. D. P., Karlin, K. D., Hodgson, K. O., Hedman, B. & Solomon, E. I. (2013). *J. Am. Chem. Soc.* **135**, 17417-17431.
- Ravel, B. & Newville, M. (2005). *J. Synchrot. Radiat.* **12**, 537-541.
- Simonne, H. D. (2019). Master thesis, Technische Universitat Munchen.
- Stöhr, J. (1992). *NEXAFS Spectroscopy*. Verlag Berlin Heidelberg: Springer-Verlag Berlin Heidelberg.
- Tamenori, Y. (2013). *J. Synchrot. Radiat.* **20**, 419-425.
- te Velde, G., Bickelhaupt, F. M., Baerends, E. J., Guerra, C. F., Van Gisbergen, S. J. A., Snijders, J. G. & Ziegler, T. (2001). *J. Comput. Chem.* **22**, 931-967.
- Tokushima, T., Horikawa, Y., Harada, Y., Takahashi, O., Hiraya, A. & Shin, S. (2009). *Phys. Chem. Chem. Phys.* **11**, 1679-1682.
- Virtanen, P. a. o. (2020). *Nat. Methods* **15**.
- Watts, B. (2014). *Opt. Express* **22**, 23628-23639.
- Watts, B., Thomsen, L. & Dastoor, P. C. (2006). *J. Electron Spectrosc. Relat. Phenom.* **151**, 105-120.
- Webb, S. M. (2005). *Phys. Scr.* **T115**, 1011-1014.
- Wilke, M., Farges, F., Petit, P. E., Brown, G. E. & Martin, F. (2001). *Am. Miner.* **86**, 714-730.
- Zheng, F., Alayoglu, S., Guo, J. H., Pushkarev, V., Li, Y. M., Glans, P. A., Chen, J. L. & Somorjai, G. (2011). *Nano Lett.* **11**, 847-853.

